

Stéphanie Baelen, Frédérique
Dewitte, Bernard Clantin and
Vincent Villeret*

Institut de Recherche Interdisciplinaire, IRI USR
3078 CNRS–Université Lille Nord de France,
Parc CNRS de la Haute Borne, 50 Avenue de
Halley, 59658 Villeneuve d'Ascq, France

Correspondence e-mail:
vincent.villeret@iri.univ-lille1.fr

Received 17 September 2013
Accepted 28 October 2013

PDB reference: secretion domain of HxuA, 4i84

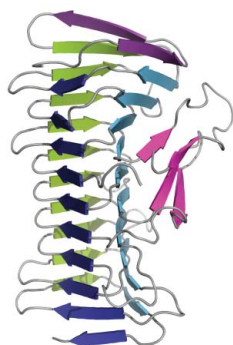
Structure of the secretion domain of HxuA from *Haemophilus influenzae*

Haemophilus influenzae HxuA is a cell-surface protein with haem–haemopexin binding activity which is key to haem acquisition from haemopexin and thus is one of the potential sources of haem for this microorganism. HxuA is secreted by its specific transporter HxuB. HxuA/HxuB belongs to the so-called two-partner secretion systems (TPSs) that are characterized by a conserved N-terminal domain in the secreted protein which is essential for secretion. Here, the 1.5 Å resolution structure of the secretion domain of HxuA, HxuA301, is reported. The structure reveals that HxuA301 folds into a β -helix domain with two extra-helical motifs, a four-stranded β -sheet and an N-terminal cap. Comparisons with other structures of TpsA secretion domains are reported. They reveal that despite limited sequence identity, strong structural similarities are found between the β -helix motifs, consistent with the idea that the TPS domain plays a role not only in the interaction with the specific TpsB partners but also as the scaffold initiating progressive folding of the TpsA proteins at the bacterial surface.

1. Introduction

Haemophilus influenzae has an absolute requirement for haem for aerobic growth. Haem–haemopexin complexes are one of the potential sources of haem for this microorganism. HxuA, a 96.3 kDa cell-surface protein, has haem–haemopexin binding activity and is the key to haem acquisition from haemopexin. HxuA belongs to the HxuCBA system, which consists of an operon encoding three proteins: HxuA, HxuB and the TonB-dependent haem receptor HxC (Cope *et al.*, 2001). HxuA, which is conserved among *H. influenzae* strains, is released at the cell surface by its transporter HxuB (Cope *et al.*, 1995), rendering the protein accessible for interaction with haem–haemopexin. Following the interaction between HxuA and haem–haemopexin, haem is released and becomes accessible to the haem receptor HxC for transport within the bacteria (Fournier *et al.*, 2011).

A key element for efficient HxuA function is thus its transport to the cell surface by its associated transporter HxuB. HxuA/HxuB belongs to the so-called two-partner secretion (TPS) pathway found in Gram-negative bacteria (Jacob-Dubuisson *et al.*, 2009). Currently, hundreds of TPS systems have been identified, mainly from large-scale sequencing initiatives, and an increasing number of them are being characterized. As implied by the name, TPS systems involve pairs of proteins: the secreted proteins are collectively called TpsA proteins (the ‘cargos’) and their outer membrane partners are collectively called TpsB proteins (the ‘transporters’). The defining feature of the TpsA proteins is the presence of a conserved, approximately 250-residue ‘TPS’ domain located at the N-terminus of the mature protein. Most TpsA proteins are large and are predicted to form extended β -helix structures (Kajava *et al.*, 2001; Kajava & Steven, 2006). TpsB partners are 60 kDa proteins that are embedded in the outer membrane and are composed of two large moieties. The periplasmic moiety is formed by two successive POTRA (polypeptide transport-associated) domains (Sánchez-Pulido *et al.*, 2003) involved in the recognition of the TpsA cargo (Hodak *et al.*, 2006; Delattre *et*



et al., 2011). The C-terminal moiety is embedded in the outer membrane and forms a 16-stranded antiparallel β -barrel that delimits a channel thought to be the translocation pore for the TpsA partner (Méli *et al.*, 2006). Schematically, the mechanistic model for two-partner secretion is as follows. Like other signal-peptide-dependent secretion pathways, the first step is the export of the TpsA preprotein across the cytoplasmic membrane by the Sec machinery, coupled with signal-peptide cleavage (Braun *et al.*, 1992; Grass & St Geme, 2000; Chevalier *et al.*, 2004). The TpsA protein transits through the periplasm in an extended conformation assisted by chaperones (Baud *et al.*, 2009) and recognizes the periplasmic domain of its cognate TpsB partner, which initiates TpsA translocation through the TpsB pore. The TpsA polypeptide progressively crosses the outer membrane and folds. Additional steps found in a subset of systems include proteolytic maturation of the TpsA protein and/or its release from the cell surface into the milieu (Domenighini *et al.*, 1990; Barenkamp & Leininger, 1992; Ward *et al.*, 1998; Aoki *et al.*, 2005).

Structure-based multiple sequence alignments of the TPS domains of TpsA proteins have revealed two distinct subsets, with FHA, ShlA, LspA, HpmA, HhdA and HecA clustered in one group (Clantin *et al.*, 2004) while HMW1A, HxuA, RscA and EtpA appear to form another more distantly related cluster (Yeo *et al.*, 2007). A similar

clustering is revealed for their associated TpsB partners (Jacob-Dubuisson *et al.*, 2009).

Structural studies of FHA/FhaC from *Bordetella pertussis* led to crystallographic determination of the secretion domain of FHA, Fha30 (Clantin *et al.*, 2004), and its membrane partner FhaC, the only TpsB structure reported to date (Clantin *et al.*, 2007). Further structural data is available on another TpsA: the crystal structure of the secretion domain of *Proteus mirabilis* HpmA (HpmA265; Weaver *et al.*, 2009) belongs to this subfamily. Only one TpsA structure has been reported for the HMW1A/HMW1B subfamily, the secretion domain of HMW1A (HMW1A-PP; Yeo *et al.*, 2007). The HxuA/HxuB system from *H. influenzae* belongs to this latter subfamily (Jacob-Dubuisson *et al.*, 2009). To date, all structures reported for TpsA secretion domains originate from proteins which function as adhesins or haemolysins in pathogenic processes, while HxuA has a unique function among TpsA proteins as an interaction protein promoting haem release from haemopexin. Despite these functional differences, HxuA is also predicted to contain an N-terminal domain required for the secretion process, while the functional domains involved in haemopexin recognition are found in the rest of the protein (Cope *et al.*, 1994, 1998; Fournier *et al.*, 2011). As a first attempt to further characterize HxuA at the structural level and gain insights into its secretion process, we produced, purified, crystallized and determined the structure of its secretion domain (HxuA301).

2. Methods

2.1. Construction of strains, protein expression and purification

The pFHxuA₃₀₁ vector was obtained as follows. A 5' segment of the *hxuA* gene encoding amino acids 1–301 without the signal peptide was amplified by PCR from *H. influenzae* Rd KW20 genomic DNA using the forward primer 5'-GCGCAAGCTTCTCGAGAA-CACCACCACCACCACCACCGGGATTGTCACAAGGTA-GCAGTGTAGTT-3' and the reverse primer 5'-GACAGATCTTTAACCATTGATATTAACGCTTTTGCTGTAAA-3'. The sequence encoding the histidine tag is shown in bold. The amplicon was purified, digested with *Xho*I and *Bgl*II restriction enzymes (Fermentas) and cloned into the pFLAG-CTS Expression Vector (Sigma–Aldrich), which contains the *ompA* signal peptide sequence upstream of the multiple cloning site.

The *hxuB* gene was amplified by PCR from *H. influenzae* Rd KW20 genomic DNA using the forward primer 5'-CCGCTC-GAGAATTAGATCGGCCAGATACTGGA-3' and the reverse primer 5'-GGAAGATCTTTAGAAAGTTTAAATCATAGA-3'. The amplicon was purified, digested with *Xho*I and *Bgl*II restriction enzymes (Fermentas) and cloned into the pFLAG-CTS Expression Vector, thus creating pFHxuB. The pCHxuB vector was obtained as follows. The *Nde*I–*Bgl*II fragment encoding the *OmpA* signal peptide and the *HxuB* gene was excised from pFHxuB and inserted into the pCOLADuet-1 vector. The integrity of all vectors was verified by DNA sequencing.

The expression vectors pFHxuA₃₀₁ and pCHxuB were co-transformed into *Escherichia coli* strain BL21(DE3)omp5 by electroporation (Prilipov *et al.*, 1998). The bacteria were grown at 310 K in 1 l LB medium supplemented with 100 μ g ml⁻¹ ampicillin and 25 μ g ml⁻¹ kanamycin. Overexpression of His₇-HxuA₃₀₁ and HxuB was induced at an OD₆₀₀ of 0.6 by the addition of 1 mM isopropyl β -D-1-thiogalactopyranoside (IPTG) and cell growth was continued for 3 h at 310 K.

After 1 h of centrifugation at 4700g, one tablet of EDTA-free protease-inhibitor cocktail (cComplete EDTA-free Protease Inhibitor

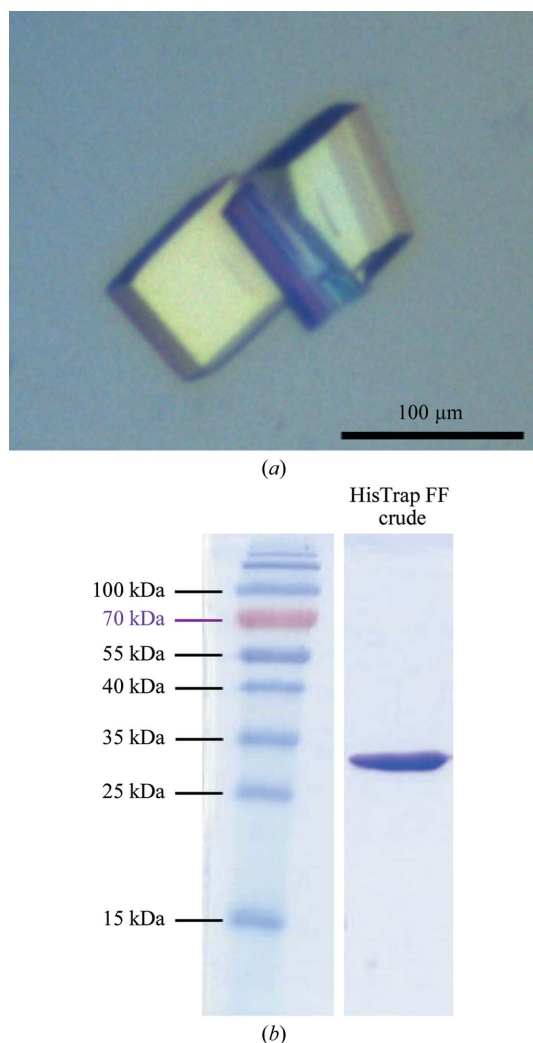


Figure 1
(a) His₇-HxuA₃₀₁ crystal. (b) SDS-PAGE gel of purified His₇-HxuA₃₀₁ (33.3 kDa).

Cocktail, Roche) and 50 mM imidazole pH 6.5 were added to the culture supernatant. The His₇-HxuA₃₀₁ protein contained in the supernatant was purified using a HisTrap FF Crude 1 ml column (GE Healthcare) equilibrated with 50 mM imidazole pH 6.5 and was eluted with 1 M imidazole pH 6.5. After elution, pure His₇-HxuA₃₀₁ was directly recovered at a concentration of 2.8 mg ml⁻¹ (Fig. 1).

2.2. Crystallization

Crystallization trials were carried out by the hanging-drop vapour-diffusion method. The conditions from The Cryos Suite screening kit (Qiagen) were investigated by mixing 1 µl protein solution and 1 µl well solution at 293 K. Initial crystallization hits were optimized to obtain suitable crystals for data collection. The best crystallization condition was 1 M imidazole pH 6.5 (from the protein solution), 0.095 M trisodium citrate pH 5.6, 19%(v/v) 2-propanol, 5%(v/v) glycerol, 12%(w/v) PEG 4000 (Fig. 1), yielding crystals that belonged to space group *P*₂₁ with unit-cell parameters *a* = 38.99, *b* = 70.84, *c* = 104.98 Å, β = 98.1°.

2.3. Data collection and processing

Prior to data collection, the crystals were briefly soaked in 0.095 M trisodium citrate pH 5.6, 19%(v/v) 2-propanol, 5%(v/v) glycerol, 19%(w/v) PEG 4000. X-ray data were collected at 100 K on the PROXIMA1 beamline at the SOLEIL synchrotron (Gif-sur-Yvette, France). The diffraction data were indexed, integrated, scaled and merged with the *XDS* package (Kabsch, 2010). The statistics of data

collection are summarized in Table 1. The volume of the unit cell suggests the presence of two molecules in the asymmetric unit.

2.4. Structure solution and refinement

The structure of the secretion domain HxuA₃₀₁ was solved by molecular replacement using *MOLREP* v.9.2 from the *CCP4* suite v.6.1.13 (Winn *et al.*, 2011). A search model based on the HMW1A-PP structure (PDB entry 2odl; Yeo *et al.*, 2007), which shares 26.9% sequence identity with HxuA₃₀₁, was prepared in which side chains were truncated to alanine using *PDBSET* from the *CCP4* suite v.6.1.13 (Winn *et al.*, 2011). Model building was performed using *ARP/wARP* v.7.1 (Langer *et al.*, 2008) coupled to the *CCP4* package, specifically using *REFMAC5* (Murshudov *et al.*, 2011). The two molecules in the asymmetric unit were treated independently during refinement. Rounds of model manipulation using *Coot* (Emsley *et al.*, 2010) interspersed with refinement using *REFMAC5* were used to complete the protein model with the addition of water molecules. The final refinement statistics are presented in Table 1.

The loops between strands β15 and β16 in monomers *A* and *B* (see Fig. 4b for β-strand numbering) are not well defined, with residues Leu126–Gln130 and Lys127–Glu134 missing in the electron-density map, respectively. Monomer *B* presents four additional poorly defined regions (residues Glu113–Asn118, Thr181–Ser185, Glu192–Ala195 and Gly217–Gln220). The overall *B* factors are 19.2 Å² for monomer *A* and 22.6 Å² for monomer *B*.

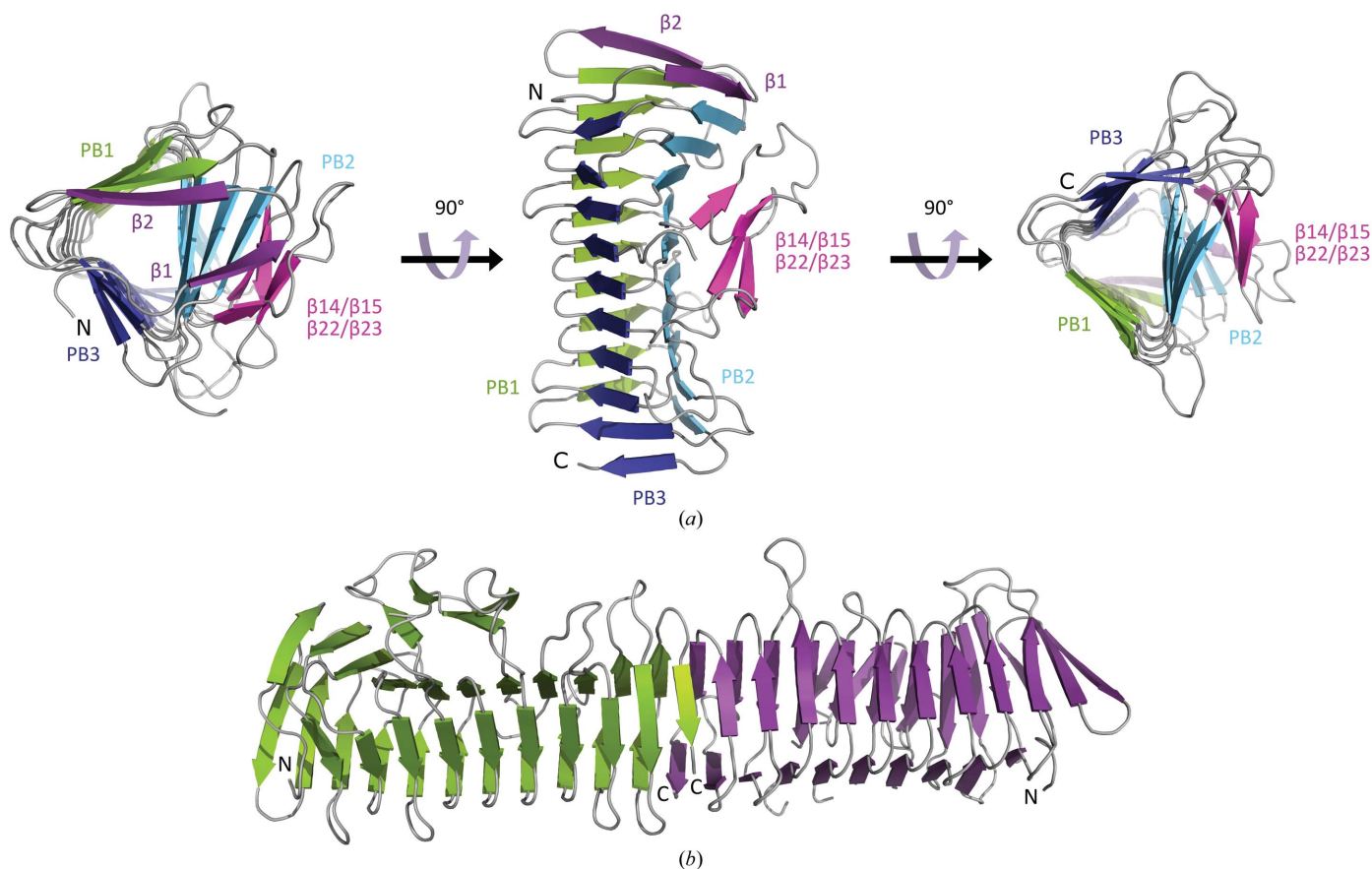


Figure 2 (a) Ribbon representations of the β-helix structure of HxuA₃₀₁. β1 and β2 are coloured purple, PB1 green, PB2 sky blue, PB3 dark blue and the extra-helical motif β14/β15–β22/β23 pink. (b) Ribbon representation of the HxuA₃₀₁ dimer corresponding to the asymmetric unit of the crystal. N- and C-terminal extremities are indicated.

3. Results and discussion

3.1. General comments and overall structure

The HxuA301 protein folds as a right-handed parallel β -helix consisting of ten coils (Fig. 2a). Each coil contributes to a complete turn of the parallel β -helix (Jenkins & Pickersgill, 2001). Like the TPS domains of FHA from *B. pertussis* and HpmA from *P. mirabilis*, HxuA301 crystallizes as a homodimeric β -helix (Fig. 2b). This dimeric organization appears to be functionally irrelevant because it results from the antiparallel β -complementation of the C-terminal last β -strands of the truncated protein. The dimensions of a monomer of HxuA301 are $50 \times 38 \times 30$ Å.

The structural motif of the right-handed parallel β -helix is made up of three parallel β -sheets named PB1, PB2 and PB3 (Fig. 2a). The coils of the β -helix become more regular from the N-terminal to the C-terminal part to finally display a triangular-shaped section. In most right-handed β -helices the hydrophobic core is shielded from the solvent by an amphipathic α -helix at the N-terminus (Jenkins & Pickersgill, 2001). However, the N-terminal capping of the HxuA301 β -helix is carried out not by an α -helix but by strands β 1 and β 2. β 1 and β 2 initiate PB2 and PB1, respectively, and represent the only antiparallel strands found in the three parallel β -sheets PB1–3.

Residues whose side chains are oriented towards the interior of the β -helix are mostly hydrophobic. In its β -helix motif, HxuA301 includes 'stacked' residues, defined as similar residues found at equivalent position in adjacent coils (Yoder *et al.*, 1993; Petersen *et al.*, 1997; Jenkins & Pickersgill, 2001). The PB1 β -sheet of HxuA301 includes two aliphatic stacks composed of six and ten residues, with the longer stack running along the entire parallel β -sheet. These stacks are composed of alanine, valine, leucine, isoleucine and methionine residues. The PB2 β -sheet of HxuA301 also includes two aliphatic stacks of six and nine residues composed of alanine, valine, leucine and isoleucine residues. Finally, PB3 includes two aliphatic stacks composed of three and eight residues comprising only valine and isoleucine. The shortest aliphatic stack is directly followed by an asparagine ladder involving residues Asn139, Asn158, Asn202 and Asn228 from β 16, β 19, β 24 and β 27, respectively. This asparagine ladder is also found in the structure of HMW1A-PP (Yeo *et al.*, 2007).

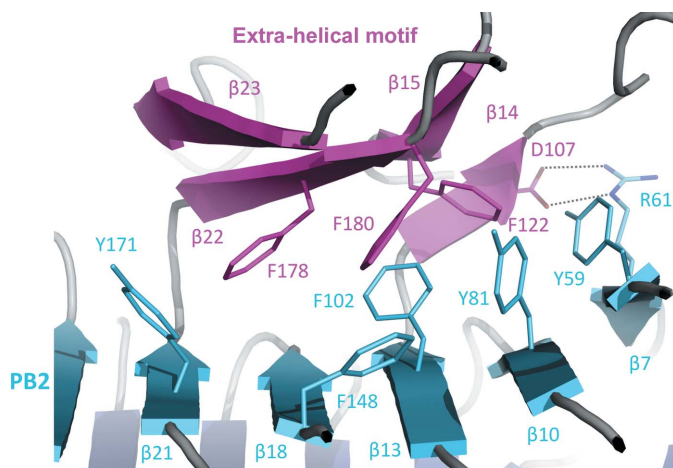


Figure 3

Close-up view of the interaction between the extra-helical motif and PB2. This motif, composed of strands β 14, β 15, β 22 and β 23, interacts with PB2 via one salt bridge (between Arg61 from β 7 and Asp107 from β 14) and via a network of aromatic-aromatic interactions involving eight residues: three tyrosines (Tyr59, Tyr81 and Tyr171) and five phenylalanines (Phe102, Phe122, Phe148, Phe178 and Phe180).

Table 1

Data-collection and refinement statistics for HxuA301 (PDB entry 4i84).

Values in parentheses are for the outermost resolution shell.

Data collection	
Unit-cell parameters (Å, °)	$a = 38.99$, $b = 70.84$, $c = 104.98$, $\beta = 98.1$
Space group	$P2_1$
Beamline	PROXIMA1, SOLEIL
Wavelength (Å)	0.98011
Temperature (K)	100
Detector	PILATUS 6M
Crystal-to-detector distance (mm)	269.63
Rotation range per image (°)	0.2
Exposure time per image (s)	0.2
Images collected	1200
Resolution (Å)	1.50 (1.59–1.50)
No. of reflections	
Observed	397746 (62011)
Unique	89861 (14222)
Crystal mosaicity (°)	0.2
Completeness (%)	99.2 (97.8)
Multiplicity	4.4 (4.4)
$R_{\text{merge}}(I)^\dagger$ (%)	3.6 (27.8)
R_{meas}^\ddagger (%)	4.0 (31.7)
$\langle I/\sigma(I) \rangle$	21.7 (4.6)
Refinement	
R_{work}^\S (%)	15.9 (23.2)
R_{free}^\P (%)	21.0 (29.4)
Mean B (Å ²)	20.9
No. of non-H atoms	
Protein	4708
Water	171
R.m.s.d.	
Bond lengths (Å)	0.027
Bond angles (°)	2.236
Ramachandran statistics †† (%)	
Preferred	97.5
Allowed	2.5
Disallowed	0.0

$^\dagger R_{\text{merge}} = \sum_{hkl} \sum_i |I_i(hkl) - \langle I(hkl) \rangle| / \sum_{hkl} \sum_i I_i(hkl)$, where $I_i(hkl)$ is the observed intensity and $\langle I(hkl) \rangle$ is the average intensity for multiple measurements. $^\ddagger R_{\text{meas}} = \sum_{hkl} [N(hkl)/[N(hkl) - 1]]^{1/2} \sum_i |I_i(hkl) - \langle I(hkl) \rangle| / \sum_{hkl} \sum_i I_i(hkl)$, where $N(hkl)$ is the number of times a given reflection has been observed. $^\S R_{\text{work}} = \sum_{hkl} ||F_{\text{obs}}| - |F_{\text{calc}}|| / \sum_{hkl} |F_{\text{obs}}|$, where F_{obs} is the observed structure factor and F_{calc} is the calculated structure factor. $^\P R_{\text{free}}$ is the same as R_{work} , except calculated using 5% of the data that were not included in any refinement calculations. †† Ramachandran values are given by the PROCHECK software from the CCP4 suite v.6.1.13 (Winn *et al.*, 2011).

Sequence analyses reveal that this asparagine motif is present in all functionally characterized TpsA proteins of this subfamily, such as the adhesin EtpA from *E. coli* and RscA from *Yersinia enterocolitica*, suggesting that this motif might be a signature of the HMW1A subfamily.

HxuA301 presents one extra β -helix motif corresponding to an antiparallel β -sheet composed of strands β 14, β 15, β 22 and β 23 and flanked against PB2 (Fig. 2a). This extra-helical motif interacts with PB2 via one salt bridge (between Arg61 from β 7 and Asp107 from β 14) and via a network of aromatic-aromatic interactions involving eight residues: three tyrosines (Tyr59, Tyr81 and Tyr171) and five phenylalanines (Phe102, Phe122, Phe148, Phe178 and Phe180) (Fig. 3). Within the HMW1A subfamily, such an extended aromatic-aromatic network is only found in HxuA. The structure of HMW1A-PP reveals a smaller aromatic network involving four residues at the interface between the extra-helical motif and PB2.

3.2. Structure comparison

HxuA301 from *H. influenzae* is the fourth TpsA secretion-domain structure to be reported to date, in addition to those of Fha30 from *B. pertussis* (PDB entry 1rwr; Clantin *et al.*, 2004), HMW1A-PP from *H. influenzae* (PDB entry 2odl; Yeo *et al.*, 2007) and HpmA265 from *P. mirabilis* (PDB entry 3fy3; Weaver *et al.*, 2009). All secretion

domains form a right-handed β -helix structure composed of three parallel β -sheets and capped by two or three β -strands (Fig. 4). This capping is specific to TpsA proteins; in other proteins adopting a right-handed β -helical fold, the hydrophobic core is shielded from the solvent by an amphipathic α -helix at the N-terminus. This specificity may result from the specialization of TPS systems for the secretion of proteins essentially composed of amphipathic β -strands.

Despite the low sequence conservation, the extra-helical motif $\beta 14/\beta 15$ – $\beta 22/\beta 23$ forming an antiparallel β -sheet is systematically

observed, with a slight difference in HMW1A-PP, in which strand $\beta 14$ is replaced by an α -helix (represented in yellow in Fig. 4). The functional role of this α -helix is still unknown. The conserved extra-helical motif may presumably be required at some stage in the mechanism of secretion. Indeed, functional studies of the FHA/FhaC system revealed that the deletion of hairpins in this region drastically reduced secretion (Hodak *et al.*, 2006).

The TpsA proteins are divided into two subfamilies: the FHA and the HMW1A subfamilies (Yeo *et al.*, 2007; Jacob-Dubuisson *et al.*,

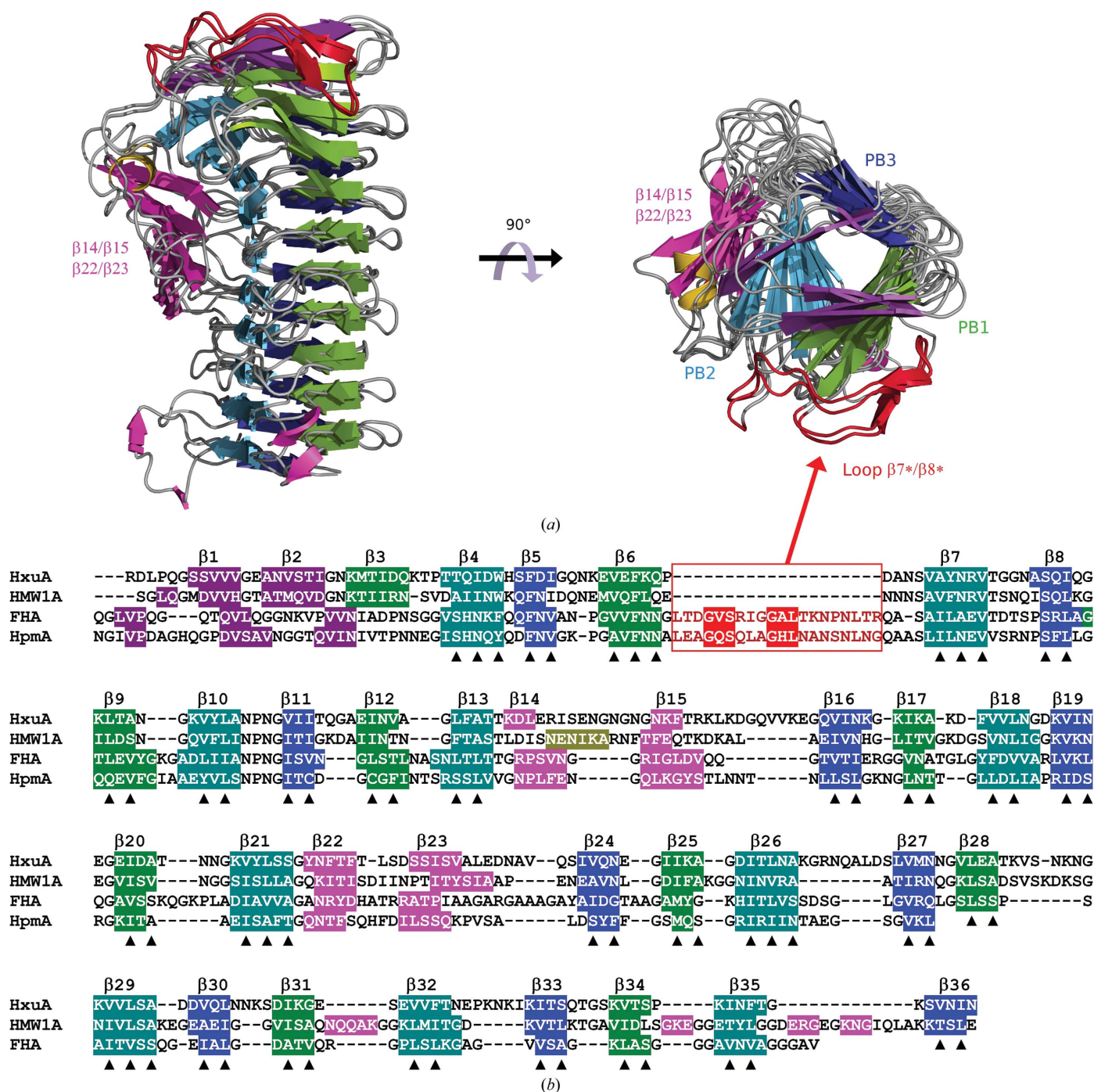


Figure 4

Structural alignment of TPS domains from TpsAs of known structure. $\beta 1$ and $\beta 2$ are coloured purple, PB1 green, PB2 sky blue, PB3 dark blue and the extra-helical motifs pink (and yellow in the case of the α -helix present in the HMW1A structure). The loop $\beta 7^*/\beta 8^*$ specific to the FHA/FhaC subfamily is coloured red. (a) Ribbon representation of the structural alignment of TPS domains from HxuA301, HMW1A (PDB entry 2odl), HpmA (PDB entry 3fy3) and FHA (PDB entry 1rwr). (b) Sequence alignment based on structural alignment of TPS domains of known structure. The residues whose side chains are oriented towards the interior of the β -helix are marked by a black triangle.

2009). In addition to the $\beta 14/\beta 15\text{--}\beta 22/\beta 23$ motif, TpsA proteins from the FHA subfamily show a second extra-helical motif made up by a long extension containing two antiparallel β -strands, designated loop $\beta 7^*/\beta 8^*$. This extension includes the NPNL motif which is conserved throughout this subfamily. Although of unknown function, this motif may play a specific role in the secretion mechanism of these TpsA proteins, for which a stable interaction between the N-terminal extremity of FHA and FhaC has been hypothesized during the secretion process (Mazar & Cotter, 2006).

HMW1A-PP, Fha30 and HpmA265 share 30.3, 14 and 14% identity, respectively, with HxuA over the 301 residues of the HxuA construct. The r.m.s. deviation calculated from residues whose side chains are oriented towards the interior of the helix (marked by a black triangle in Fig. 4b) is 0.55 Å between HxuA301 and HMW1A-PP, 1.41 Å between HxuA301 and HpmA265 and 1.29 Å between HxuA301 and FHA30. Thus, despite limited sequence identity, strong structural similarities are found between the β -helix motifs of TpsA proteins.

We thank the PROXIMA1 beamline staff for support during data collection. SB is supported by a PhD fellowship from the CNRS. FD, BC and VV are researchers from the CNRS. This work has been supported by the CNRS, ANR grant DYN FHAC (2010–2014), the Region Nord-Pas-de-Calais (France) and the CPER–CIA.

References

- Aoki, S. K., Pamma, R., Hernday, A. D., Bickham, J. E., Braaten, B. A. & Low, D. A. (2005). *Science*, **309**, 1245–1248.
- Barenkamp, S. J. & Leininger, E. (1992). *Infect. Immun.* **60**, 1302–1313.
- Baud, C., Hodak, H., Willery, E., Drobecq, H., Loch, C., Jamin, M. & Jacob-Dubuisson, F. (2009). *Mol. Microbiol.* **74**, 315–329.
- Braun, V., Hobbie, S. & Ondracek, R. (1992). *FEMS Microbiol. Lett.* **79**, 299–305.
- Chevalier, N., Moser, M., Koch, H.-G., Schimz, K.-L., Willery, E., Loch, C., Jacob-Dubuisson, F. & Müller, M. (2004). *J. Mol. Microbiol. Biotechnol.* **8**, 7–18.
- Clantin, B., Delattre, A.-S., Rucktooa, P., Saint, N., Méli, A. C., Loch, C., Jacob-Dubuisson, F. & Villeret, V. (2007). *Science*, **317**, 957–961.
- Clantin, B., Hodak, H., Willery, E., Loch, C., Jacob-Dubuisson, F. & Villeret, V. (2004). *Proc. Natl. Acad. Sci. USA*, **101**, 6194–6199.
- Cope, L. D., Love, R. P., Guinn, S. E., Gilep, A., Usanov, S., Estabrook, R. W., Hrkál, Z. & Hansen, E. J. (2001). *Infect. Immun.* **69**, 2353–2363.
- Cope, L. D., Thomas, S. E., Hrkál, Z. & Hansen, E. J. (1998). *Infect. Immun.* **66**, 4511–4516.
- Cope, L. D., Thomas, S. E., Latimer, J. L., Slaughter, C. A., Müller-Eberhard, U. & Hansen, E. J. (1994). *Mol. Microbiol.* **13**, 863–873.
- Cope, L. D., Yogeve, R., Müller-Eberhard, U. & Hansen, E. J. (1995). *J. Bacteriol.* **177**, 2644–2653.
- Delattre, A.-S., Saint, N., Clantin, B., Willery, E., Lippens, G., Loch, C., Villeret, V. & Jacob-Dubuisson, F. (2011). *Mol. Microbiol.* **81**, 99–112.
- Domenighini, M., Relman, D., Capiou, C., Falkow, S., Prugnola, A., Scarlato, V. & Rappuoli, R. (1990). *Mol. Microbiol.* **4**, 787–800.
- Emsley, P., Lohkamp, B., Scott, W. G. & Cowtan, K. (2010). *Acta Cryst.* **D66**, 486–501.
- Fournier, C., Smith, A. & Delepelaire, P. (2011). *Mol. Microbiol.* **80**, 133–148.
- Grass, S. & St Geme, J. W. III (2000). *Mol. Microbiol.* **36**, 55–67.
- Hodak, H., Clantin, B., Willery, E., Villeret, V., Loch, C. & Jacob-Dubuisson, F. (2006). *Mol. Microbiol.* **61**, 368–382.
- Jacob-Dubuisson, F., Villeret, V., Clantin, B., Delattre, A.-S. & Saint, N. (2009). *Biol. Chem.* **390**, 675–684.
- Jenkins, J. & Pickersgill, R. (2001). *Prog. Biophys. Mol. Biol.* **77**, 111–175.
- Kabsch, W. (2010). *Acta Cryst.* **D66**, 125–132.
- Kajava, A. V., Cheng, N., Cleaver, R., Kessel, M., Simon, M. N., Willery, E., Jacob-Dubuisson, F., Loch, C. & Steven, A. C. (2001). *Mol. Microbiol.* **42**, 279–292.
- Kajava, A. V. & Steven, A. C. (2006). *Adv. Protein Chem.* **73**, 55–96.
- Langer, G., Cohen, S. X., Lamzin, V. S. & Perrakis, A. (2008). *Nature Protoc.* **3**, 1171–1179.
- Mazar, J. & Cotter, P. A. (2006). *Mol. Microbiol.* **62**, 641–654.
- Méli, A. C., Hodak, H., Clantin, B., Loch, C., Molle, G., Jacob-Dubuisson, F. & Saint, N. (2006). *J. Biol. Chem.* **281**, 158–166.
- Murshudov, G. N., Skubák, P., Lebedev, A. A., Pannu, N. S., Steiner, R. A., Nicholls, R. A., Winn, M. D., Long, F. & Vagin, A. A. (2011). *Acta Cryst.* **D67**, 355–367.
- Petersen, T. N., Kauppinen, S. & Larsen, S. (1997). *Structure*, **5**, 533–544.
- Prilipov, A., Phale, P. S., Van Gelder, P., Rosenbusch, J. P. & Koebnik, R. (1998). *FEMS Microbiol. Lett.* **163**, 65–72.
- Sánchez-Pulido, L., Devos, D., Genevrois, S., Vicente, M. & Valencia, A. (2003). *Trends Biochem. Sci.* **28**, 523–526.
- Ward, C. K., Lumley, S. R., Latimer, J. L., Cope, L. D. & Hansen, E. J. (1998). *J. Bacteriol.* **180**, 6013–6022.
- Weaver, T. M., Hocking, J. M., Bailey, L. J., Wawrzyn, G. T., Howard, D. R., Sikkink, L. A., Ramirez-Alvarado, M. & Thompson, J. R. (2009). *J. Biol. Chem.* **284**, 22297–22309.
- Winn, M. D. *et al.* (2011). *Acta Cryst.* **D67**, 235–242.
- Yeo, H.-J., Yokoyama, T., Walkiewicz, K., Kim, Y., Grass, S. & St Geme, J. W. III (2007). *J. Biol. Chem.* **282**, 31076–31084.
- Yoder, M. D., Lietzke, S. E. & Jurnak, F. (1993). *Structure*, **1**, 241–251.